Supplementary Data

Metal-Induced Self-Assembly of Peroxiredoxin as a Tool for Sorting Ultrasmall Gold Nanoparticles into One-Dimensional Clusters

Matteo Ardini, Francesco Giansanti, Luana Di Leandro, Giuseppina Pitari, Annamaria Cimini, Luca Ottaviano, Maurizio Donarelli, Sandro Santucci, Francesco Angelucci, and Rodolfo Ippoliti

1 Experimental

1.1 Thermal treatment

The 6His-*Sm*PrxI thermal resistance was investigated by exposure to extreme heating conditions. First, short-term heating treatment was performed by incubating a 20 μM protein sample for 10 min at 40, 60, 70 and 75 °C in a water bath under shacking. In parallel, an analogous sample was prepared and exposed to 75 °C for 10, 30, 60 and 120 min. After treatment, samples were centrifuged 10 min at 10000 rpm and analyzed by GFC**.**

1.2 Disassembly of the protein-AuNP adducts

Three different conditions were applied to induce release of the protein-bound nanoparticles: 1) imidazole was used as histidine-specific competitor for metal binding and added to the protein-gold mixture at concentration 200-400 mM; the resulting solution was then incubated at least 1 h at room temperature under shaking; 2) alternatively, the metal binding histidine residues (pK_a= 6.0) were protonated through mild acidification to pH 5.0 using 3 M acetate buffer; 3) partial nanoparticle release and conversion of the AuNP-HMW adducts into the LMW ones were also accomplished

through dilution of the protein-gold mixture according to the metastable behavior of the AuNP-LMW and HMW species.

1.3 AuNPs conjugation to the 6His-*Sm*PrxI_C48S mutant protein

A reaction mixture containing 30 µM mutant protein, 0.1 equivalents AuNPs and 20 mM imidazole was incubated overnight at 22 °C under shaking. The resulting mixture was then centrifuged 10 min at 10000 rpm and the supernatant analyzed by GFC.

2 Figures and captions

M R G S H H H H H H G M A S M T G G Q Q M G R D L Y D D D D K D R W G S T M V L
L P N R P A P E F K G Q A V I N G E F K E I C L K D Y R G K Y V V L F F Y P A D
F T F V C P T E I I A F S D Q V E E F N S R N C Q V I A C S T D S Q Y S H L A W
D N L D R K S G G L G H M K I P L L A D R K Q E I S K A Y G V F D E E D G N A F
R G L F I I D P N G I L R Q I T I N D K P V G R S V D E T L R L L D A F Q F V E
K H G E V C P V N W K R G Q H G I K V N Q K

Figure S1. Amino acid sequence of the engineered 6His-*Sm*PrxI monomer. The N-terminal His-tail is in bold; the histidine (H) and aspartate (D) metal binding residues are in boxes.

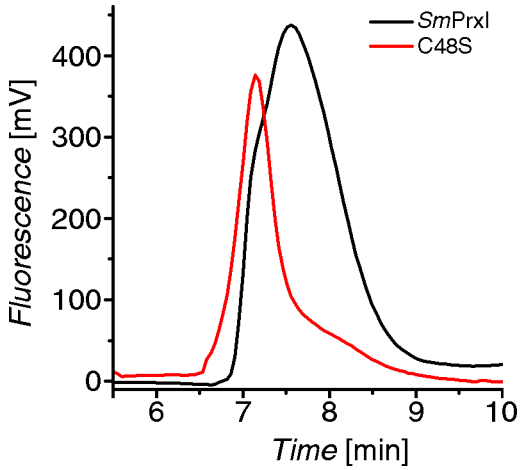

Figure S2. GFC elution behavior of the nickel-induced 6His-*Sm*PrxI aggregates compared to the self-assembling 6His-*Sm*PrxI_C48S mutant. The elution profiles partially overlap each other at high molecular weight fractions suggesting that either the wild-type and the mutant protein form aggregate complexes with comparable molecular weights.

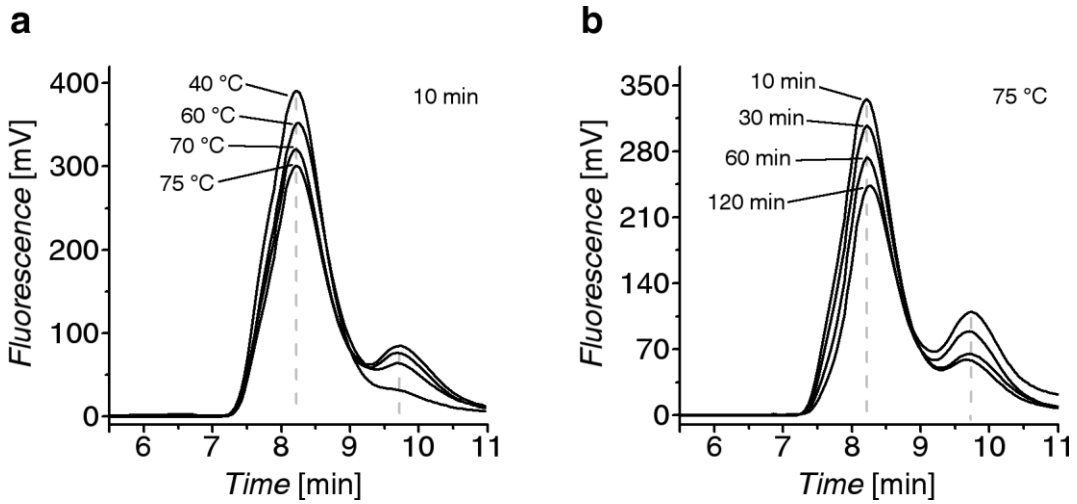

Figure S3. Thermal stability of 6His-*Sm*PrxI against heating treatments. a) Short-term (10 min) exposure to increasing temperatures (40-75 °C) does not alter the LMW oligomer organization of the protein; with increasing the temperature, some additional species ascribable to dimer molecules slowly raise. b) Similarly, during extended (10-120 min) exposure to high temperature (75 °C) 6His-*Sm*PrxI maintains its structural stability. In both cases, at least 80% of the initial fluorescence signal is always recorded indicating that no significant protein loss occurs.

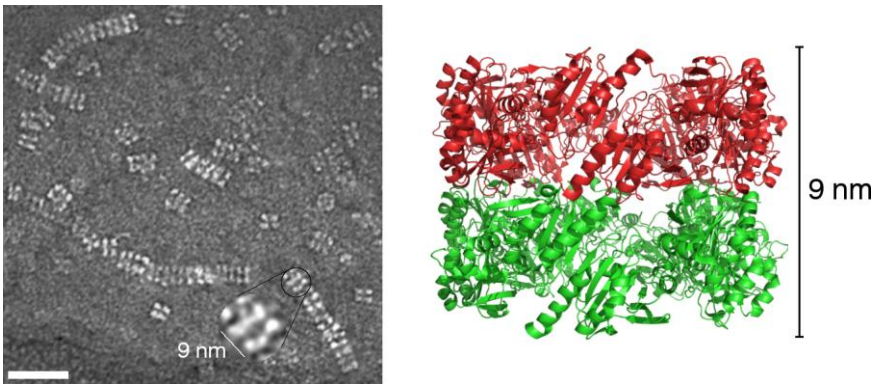

Figure S4. Comparison between TEM and crystallographic data of the *Sm*PrxI HMW stacks. The nickel-induced 6His-*Sm*PrxI nanotubes (left) show a mean value of the ring-ring proximal distance of about 9 nm which well agrees with that obtained from the crystal structure of the HMW species (right, PDB code: 3ZVJ). Scale bar corresponds to 40 nm.

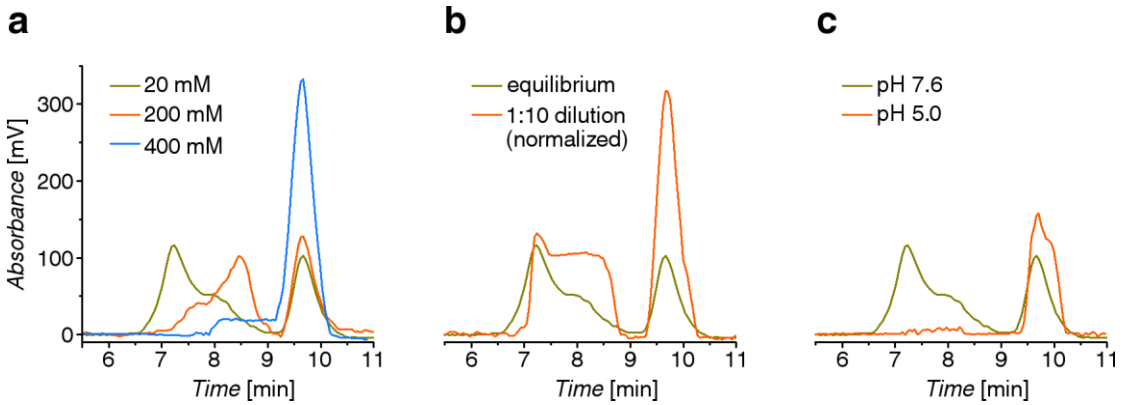

Figure S5. AuNPs incorporation under different conditions. a) Incubation to increasing imidazole concentrations leads to reduction of bound AuNPs; this effect is ascribable to the competition for metal binding between the imidazole molecules and the His-tails protein N-terminal regions. b) The relative amounts of the gold-protein fractions and the free AuNPs changes upon dilution of the gold-protein mixture, indicating that the system is under dynamic equilibrium. c) According to the nature of the metal-histidine interactions, acidification of the gold-protein mixture leads to nanoparticles release because of proton-mediated displacement of the nickel ions from the histidine residues. For clarity, graphs report only the gold optical absorbance without the respective protein fluorescence.

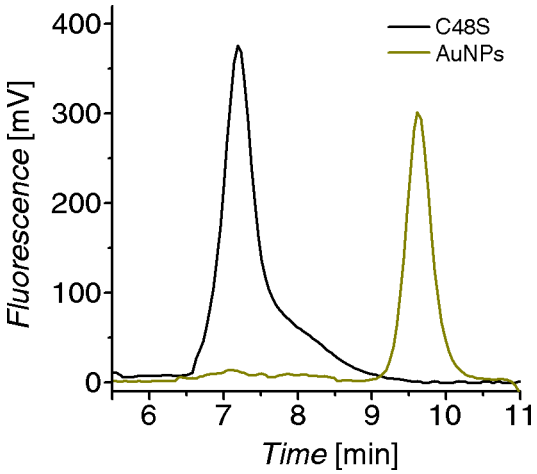

Figure S6. Lack of incorporation of the AuNPs within the self-assembling 6His-*Sm*PrxI_C48S mutant protein. GFC experiments show that 6His-*Sm*PrxI_C48S does not co-elute with the gold nanoparticles indicating that the mutant protein fails in binding efficiently the gold. The graph refers to a 24 h reaction. Changing the stoichiometry of reaction does not alter the results (data not shown). As yellow line the absorbance at 420 nm of the AuNPs is reported.

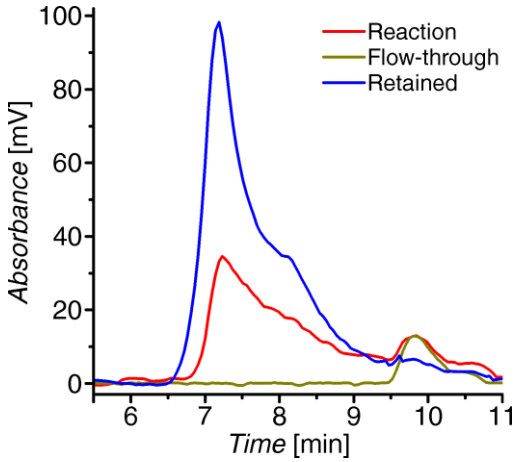

Figure S7. Prx decamers (3μM) and an equivalent amount of AuNPs (commercially available from Nanoprobes, Yaphank, NY, USA) were incubated at 37 °C for 6 hours. The resulting reaction mixture was analyzed by GFC which demonstrates the presence of AuNP-HMW and AuNP-LMW species together with the unbound fraction of AuNPs (red chromatogram). The mixture was then introduced into a diafiltration device (MW cut-off 100 kDa, Millipore) and after spinning at 5000 rpm for 5 min, both the flow-through and the retained sample were again analyzed by GFC. The flow-through shows the presence of only unbound AuNPs (yellow chromatogram) in the same amount of the crude reaction (red chromatogram) while the retained sample displays higher concentration of both AuNP-LMW and AuNP-HMW species free from unbound AuNP (blue chromatogram).

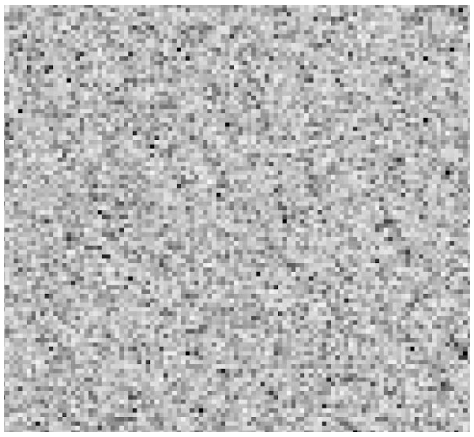

Figure S8. EFM control measurement. The micrograph has been taken on the same portion of the support displayed in Figure 7 panel A of the main text. As shown, no phase reaction is observed at 0 V potential voltage for AuNP-LMW adduct.

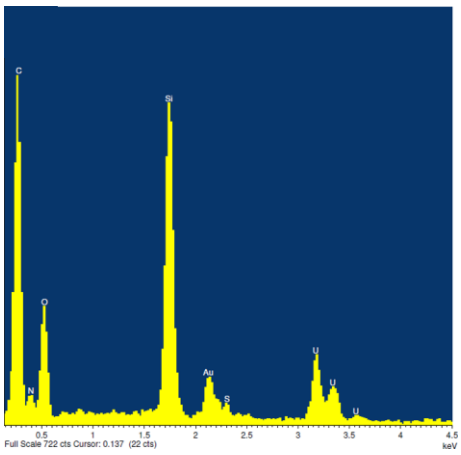

Figure S9. EDX spectrum of AuNP-HMW species, deposited on a grid made of silicon dioxide and carbon. The sample, stained with uranyl acetate, has been firstly investigated with TEM (see Figure 6e of the main text) and then with EDX spectroscopy, using a SEM (Philips XL-30-CP) equipped with a thin-window EDAX DX4 system for X-ray microanalysis by Energy Dispersion spectrometry. The spectrum shows spectral features of sulfur and nitrogen which can be specifically ascribed to the protein components, while the silicon peak unequivocally belongs to the microscopy grid; the peaks of carbon and oxygen cannot unequivocally assigned being common to several species of the sample. The gold peak (M line at 2.12 keV) of the AuNPs is present together with that of uranium (M series at 3.17, 3.34, and 3.57 keV) of the negative stain, which is specifically bound to the protein.